Optimization of Lamb Wave Actuating and Sensing Materials for Health Monitoring of Composite Structures

Seth S. Kessler*[a], Christopher T. Dunn[b]
[a] Metis Design Corporation, 46 Second St., Cambridge, MA, USA 02141
[b] Massachusetts Institute of Technology, 77 Massachusetts Ave., Cambridge, MA USA 02139

ABSTRACT

In a continuing effort to examine the effectiveness of Lamb wave methods for the health monitoring of composite structures, this paper presents the conclusions of an analytical and experimental study optimizing piezoelectric patches to detect damage within composite laminates. Previous research has demonstrated the ability of Lamb waves to provided useful information about the presence of damage in simple narrow coupons, and they have yielded the possibility of estimating severity and location of damage as well. During the course of this NRO funded research program, several types of piezoelectric materials in various configurations were analyzed in order to produce the highest force actuator and best resolution sensor at the lowest power level. Consideration was also placed towards directionality of wave propagation, and durability, reliability and reproducibility of the sensing patch itself. Experiments were then carried out on narrow coupon laminates to qualify and tune these actuating/sensing patches. New algorithms were used to filter and decompose the resulting signals to more efficiently detect the presence of damage for automated use, and gather information relating to the damage type, severity and location. SHM technologies will enable condition-based maintenance for efficient structural design, will reduced overall life-cycle costs, and eliminate scheduled inspections

Keywords: Structural Health Monitoring, Lamb waves, Polymer-matrix composites, piezoelectric, NDE

1. INTRODUCTION

The benefits of composite materials in modern air and spacecraft are well known: compared to metals, composites can have lighter weight, superior structural properties, and the capability to be readily formed into custom shapes to meet unique requirements. Non-destructive evaluation (NDE) techniques, however, have been problematic to employ. Heritage techniques such as the "tap-test", commonly used to check fiberglass payload fairings, were extremely technician-sensitive and statistically unreliable. Currently successful laboratory non-destructive testing methods, such as X-radiographic detection and C-scans, are impractical for service inspection of large integrated subsystems. More current techniques such as acoustic emission testing, modal wave surveys, thermographs, and X-rays are not easy to employ due to the size and complexity of the support equipment required [1]. Worse yet, these techniques are difficult to employ once the composite item in question has been integrated into an assembly and access to the item in question has become limited. The principal problem is determining the extent and nature of suspected structural anomalies in composite structure when visual inspections may not suffice, and more perceptive NDE techniques are not practical. These structural anomalies may include delaminations, "kissing debonds", fiber fractures, or matrix cracks caused by misuse, impacts or cyclic fatigue. In many cases, it's extremely difficult to isolate the suspected item to conduct more detailed check since the disassembly of critical subsystems could compromise critical factory alignments with negative impacts to mission success. It is clear that new approaches for inspection of composites need to be developed [2]. To resolve this issue, Metis Design Corporation (MDC) have been working with MIT and the NRO to developed a structural health monitoring (SHM) system for damage detection in composite materials, using Lamb waves driven and received by piezoelectric wafers.

* skessler@MetisDesign.com; phone 1-617-661-5616; fax 1-801-761-6995, www.MetisDesign.com

The basis for much of the work reported in this paper is a continuation of the authors' previous Lamb wave research, "PiezoElectric-Based In-Situ Damage Detection of Composite Materials for Structural Health Monitoring Systems" [3]. During this investigation several potential NDE methods and SHM components were investigated for detecting damage in composite materials. Other publications by the author on this same subject can be found in several journals and conference proceedings, focusing on the different detection methods and system architectures [4-11]. The conclusion of this research was that Lamb waves offered the best resolution to range ratios for the detection of damage in large composite structures. Lamb waves are a form of elastic perturbation that can propagate in a solid plate with free boundaries [12-14]. The present work utilizes piezoelectric patches to excite the first anti-symmetric Lamb wave (A_0 mode) in composite specimens. Using the Lamb wave method, results have been presented for applications to quasi-isotropic graphite/epoxy laminate and sandwich panel specimens containing representative damage modes, including delaminations, transverse ply cracks and through-holes. Piezoelectric wafers affixed with thermoplastic tape were used as actuators and sensor, so that the specimens could be re-used for testing using other non-destructive methods. During prior research, the most significant result was a "blind test" of composite sandwich specimens. Four high density aluminum beam specimen were tested, one of which had a known disbond in its center, while of the remaining three specimens it was unknown which contained the circular disbond and which two were the undamaged controls. By comparing the four wavelet coefficient plots, one could easily deduce that the two control specimens are the ones with significantly greater energy in the transmitted signals, while the third specimen (Control C) obviously has the flaw that reduces energy to a similar level to that of the known delaminated specimen. This test serves as a testament to the viability of the Lamb Wave method being able to detect damage in at least simple structures.

Lamb wave techniques have proven to provide more reliable information about the presence, severity and type of damage in a complex specimen than other methods. They have also demonstrated suitability for health monitoring applications since they have a large coverage area, can be applied with low power and conformable actuators and sensors, and they can provide useful information about the state of a structure during operation. Now that this system has been successfully demonstrated in laboratory conditions, during the course of this present work, Metis Design and MIT have analytically and experimentally investigated the Lamb wave infrastructure to optimize the sent and received signal for efficient and accurate results. These components include the piezoelectric sensors and actuators, the mechanical and electrical connections and the configuration necessary to integrate them. New algorithms have also been written to yield less subjective interpretation of system results.

2. SENSOR SELECTION

During the course of previous research, PZT-5H piezoceramic rectangular actuators and sensors had been used to drive Lamb wave modes and sense their transmitted and reflected displacements. The original PZT material and basic geometry had been chosen as consequence to availability at the time of those experiments. The purpose of the present research was to analytically derive figures of merit that could be used to properly select optimal actuator and sensor materials and geometries. Additionally, the mechanical and electrical connections of the actuators and sensors were analyzed. Following each of these analyses, experiments were performed to validate these results, and to conclusively select the ideal piezoceramic configuration for SHM application. This first section focuses on the piezoceramic sensors that were used to detect the Lamb waves. While much literature exists specifying optimal actuator parameters, little work can be found investigating their complementing sensors [13, 14]. The following section provides derivations that can be used to formulate figures of merit to select an optimal sensing material for Lamb wave techniques, and the corresponding geometry. Experimental results are then provided that seek to validate these theoretical calculations, and the final sensor material and geometry described.

2.1. Theoretical calculations

The piezoelectric sensor was designed to use the 3-1 piezoelectric coupling to output an open circuit voltage in response to strain. There were several desirable attributes for the piezoelectric sensor. First, the stiffness of the sensor needed to be minimized to maximize the amplitude of the strain wave passing through it. Second, to maximize the average strain in the actuator, and therefore maximize the average voltage output, the length of the sensor needed to be $0.5n^*\lambda$ where λ is the wavelength of the wave passing through the structure and n is an odd integer. Third, the sensor

needed a small impedance, such that the impedance of the system used for the voltage measurement appears large compared to the sensor, so that the sensor outputs an open circuit voltage. For example if the voltage measurement system was an oscilloscope, the impedance of the sensor needed to be much less than the typical input impedance of an oscilloscope (1 MΩ impedance). Fourth, the sensor needed to have material properties such that g_{31}*Y_{11}^{D} is maximized where g_{31} is 3-1 piezoelectric "voltage" coefficient, and Y_{11}^{D} is the open circuited Young's modulus. A list comparing the properties and figures-of-merit for several potential piezoceramic sensing materials can be seen in **Figure 1**.

2.2. Experimental results

Using this analysis, several candidate sensor materials of various geometries were tested. EBL #1,2,3,5 and 23 from Staveley Sensors were purchased, at a variety of widths, lengths and thickness. A single PZT actuator was placed in the center of a circular CFRP plate, and each of the candidate rectangular sensors were placed equidistantly around the circumference of the plate. A continuous sine sweep between 1 kHz and 250 kHz was sent to the actuator to propagate Lamb waves of various speeds towards the sensors as data was collected from each. Using the results from the analysis, and the results from the testing, disk sensors with a 12 mm diameter and 254 μm (10 mil) thickness composed of EBL #2 (Navy II or PZT-5A) were chosen. Several of the PZT sensors had the same maximum peaks, as seen in **Figure 2**, however the PZT-5A had the highest mean peak value, as well as the widest peak bandwidth, so that the high output could be seen at a broader range of frequencies.

3. ACTUATOR SELECTION

As described in the previous section, theoretical calculations were carried out to predict the optimal type of piezoceramic material for actuation, and the corresponding geometry. The actuators used during prior research were PZT-5H wafers machined into 12x6 mm rectangles. Using a driving amplitude of 10V at 15 kHz, a voltage of about 20 mV was produced by the stress waves impinging under the sensors. However, the noise level observed during these experiments was on the order of 5 mV, a substantial percentage of the actual signal. Increasing the output voltage was not a viable option, since the power requirements of the system are proportional to V^2 [$P=2\pi f CV^2$], and the eventual goal was to implement this type of actuator in an SHM system. Therefore, the following analysis was carried out to attempt to increase the signal-to-noise ratio of the actuator/sensor system without changing the voltage level or operating frequency, by choosing a material with increased strain per volt properties and specifying a resonant geometry. Following the theoretical section, experimental results are provided along with the details of the actuator material and geometry selected for future Lamb wave testing.

3.1. Theoretical calculations

PZT piezoceramic actuators were chosen for the present research due to their high force output at relatively low voltages, and their good response qualities at low frequencies. The actuator was designed to use 3-1 actuation to output a strain in response to voltage. There were two major criteria when choosing the actuator: to maximize the strain in the structure per unit volt, and to keep the magnitude of the power delivered by the function generator below 50 mW. To maximize the strain per volt induced in the structure one should maximize:

$$\frac{e_{31}^{P}}{\left(c_{11}^{P}+c_{12}^{P}\right)h_{P}+\left(Q_{11}+Q_{12}\right)h_{s}} \tag{1}$$

Where e^P is the planar piezoelectric "stress" coefficient, h_P is the thickness of the piezoelectric material, h_S is the thickness of the structure, and c^P and Q are the stiffness of the structure and the actuator respectively. To minimize the power delivered by the function generator one should minimize the admittance of the actuator:

$$\varepsilon_{33}^{P}\left(\frac{1}{h_{P}}+\frac{2\,c_{11}^{P}\left(k^{P}\right)^{2}}{\left(c_{11}^{P}+c_{12}^{P}\right)h_{P}+\left(Q_{11}+Q_{12}\right)h_{S}}\right) \tag{2}$$

Where k^P is the planar coupling coefficient and ε^P is the planar permittivity. A list comparing the properties and figures-of-merit for several potential piezoceramic actuating materials can be seen in **Figure 3**.

Waves propagate parallel to each edge of the actuator, i.e. longitudinally and transversely for a rectangular patch and circumferentially from a circular actuator. The width of the actuator in the propagation direction is not critical, however the wider it is, the more uniform the waveform created. As cited in the literature though, there is an important sinusoidal relationship between actuating frequency and actuator length [15, 16]. In the direction of propagation the desired actuator length 2a for most efficient signal is:

$$2a = \lambda\left(n + \frac{1}{2}\right) = \frac{c_p}{f}\left(n + \frac{1}{2}\right) \quad \text{for n} = 0, 1, 2, 3... \tag{3}$$

This value of 2a could either be a rectangular side length or the diameter of a circular actuator. This equation could also be used to determine actuator minimum dimensions, in order to inhibit waves from propagating in undesired directions.

3.2. Experimental results

After the sensor tests, a series of test were performed to ascertain which was the best actuating material. Based upon the analysis, the same set of EBL piezoceramic wafers were used as for the sensor tests, in order to test a broad range of material property combinations. Using the same setup as described previously, each of the wafers that had been used for sensing were reversed to produce a actuating signal, which would then be received by the central PZT wafer. Both EBL #1 and #23 were placed in the center of the plate for different series of tests to verify the results, which the results can be seen in **Figure 4**. Based on these results and the analysis thick disk actuators composed of EBL #2 were chosen, with a 25 mm outer-diameter, a 12 mm inner-diameter and thickness of 254 μm (10 mil). While the EBL #2 (PZT-5A) did not have the highest mean peaks for these tests, they were very close to the top performers, however have the added benefit of being the most temperature stable, so yield more reliable results in real operating environments. Actuators running at resonance were also analyzed, however due to their large size (3-4" for 25 kHz), and small frequency bandwidth (about 250 Hz for EBL#2 with resonance at 25 kHz), it was decided not to actuate at resonance.

4. MECHANICAL AND ELECTRICAL CONFIGURATIONS

An area that has not been explicitly investigated in the literature is the influence of the electrical and mechanical connections on the performance of piezoceramic actuators and sensors. Previous research performed by the authors had used a copper bottom electrode connected to the piezoceramic wafer using silver epoxy, and 3M Thermobond thermoplastic tape to adhere to the surface of the specimen. While this setup produced reasonable results, it was not very robust or reproducible. The desired functionality of these connections was to produce a consistent actuator/sensor patch for Lamb waves with a flat, semi-pliable surface that could easily bond rigidly to composite surfaces and be removed without damaging the structures. The following sections detail the analytical and experimental investigation of these parameters, as well as delineating the final configuration of the actuator/sensor patches selected for future Lamb wave testing.

4.1. Mechanical connections

In order to adhere the piezoceramic material to the electrical conductor and the conductor to the structure, a thin electrically conducting polymer adhesive was used. This adhesive provided an electrical path between conductor and underside of actuator/sensor, and grounded the conductor to the structure. The adhesive was chosen based upon several criteria. First, the adhesive was chosen so that the actuator/sensor could be removed from the structure, without marring the surface. This was so if damage was detected in the structure, the sensors could be removed for a potential repair. Thermoplastic film, double-sided tape, and thermoset adhesives that can be removed using solvents were candidate materials. Second, the material needed to have a low application temperature for easy installation, and to prevent depoling of the piezoelectric materials. Piezoelectric materials should not be subjected to temperatures above half the Curie temperature in Celsius to prevent depoling. Third, the material needed a uniform thickness so that different sensor and actuator would have the same response when exposed to stimuli. Based upon this criterion, only film adhesives could be used, as opposed to liquid adhesives. Finally the adhesive was chosen such that G / h^2 is minimized, where G is the shear modulus and h is the thickness, based on a shear lag analysis [15]. Since shear modulus data is not measured typically by the manufacturer, several adhesives were tested to experimentally determine which adhesive provided the largest voltage gain between the actuator and a sensor bonded to a plate. The experimental procedure was similar to that

to validate the sensor and actuator calculations was followed to compare each of the adhesives considered. A circular PZT actuator was placed in the center of a circular CFRP plate, and PZT sensors were placed equidistantly around the edge. A signal was sent to the central actuator, and signal output strength was measured at each of the PZT sensors that were bonded by various adhesives. Based upon these criteria and the testing, 3M 9703 electrically conductive tape 50.8 μm (2 mil) thick chosen for the adhesive.

4.2. Electrical connections

An electrical conductor was needed to provide a conductive path between the ground wire and the underside of the actuator and sensor and the ground. There were several desirable attributes when choosing an electrical conductor. First, the conductor needed to have a minimum in-plane stiffness to maximize actuation. The in-plane stiffness of the conductor is proportional to $E\,h$, where E is the Young's modulus of the electrical conductor and h is the thickness. Second, it was desirable for the material to be a metal such that a cable BNC connector can be soldered to it easily. Using a short cable BNC connector the electrical noise can be minimized. Third, the conductor needed to be thick enough so that it did not tear when the wires were inadvertently tugged. Fourth, the conductor needed to possess a small resistance such that the resistance is small compared to the function generator output impedance, and the impedance of sensor and actuator. Typically, a function generator has an output impedance of 50 Ω, and a piezoelectric sensor with a capacitance of 10 – 25 nF driven at 50 kHz has an impedance of 318-127 Ω respectively. Thus, it was decided that the resistance of the conductor should be less than 1 Ω. Given these attributes, a 25.4 μm (1 mil.) thick brass alloy 260 shim stock was chosen for conductor. This shim was 81% less stiff than a 127 μm (5 mil.) copper shim previously used [3]. Thinner brass shims were tested, however they had a tendency to tear when the ground wire was inadvertently tugged. Tests were also performed using magnet wire, however the wire was so thick that a very large amount of adhesive was required to bond the piezoelectric materials to the structure, which was undesirable.

4.3. Overall selected configuration

At the conclusion of the three sets of experiments described in the previous sections, a final overall optimal configuration was selected for testing future composite specimens using the Lamb wave method. Using the rational described earlier, PZT-5A was selected for both the actuating and sensing materials. During previous experimentation, side-by-side actuators and sensors had been attempted to measure the reflected signal, however that did not yield good results. Attempts were also made to use a self-sensing circuit in order to use the driving piezoceramic wafer to measure the reflected waves as well, however this concept only had limited success due to the changing capacitance with the sensor with frequency and the poor tolerances between PZT specimens. For the present research, a PZT disk circumscribed by a PZT ring was used for an actuating and sensing scheme with good success. All four combinations were experimentally tested (disk-disk, ring-ring, ring-disk, and disk-ring) and it was determined that the best signal was obtained by using the rings as the actuator and the disks on either side of the damage as the sensors. The reverse scheme yielded the next best results. The disk had a 12mm diameter as calculated for optimal sensing, and the ring had an overall diameter of 25mm with a true width of 6mm. The PZT wafers were bonded to the brass shim electrode using the 3M electrically conductive tape with a small separation between them. This thermoplastic tape requires no heat for adhesion, and just a small amount of uniform pressure. This assembly was then bonded to the structure using a similar 3M tape that was not conductive. Lastly, the electrical connections were made by soldering BNC cables to the nickel electrode on top of each PZT and a tab on the brass shim, forming a common ground. A schematic of this set-up can be seen in **Figure 5** and a photograph of the assembly as tested in **Figure 6**. The results collected using was then decomposed using the algorithms presented in the following section.

5.ALGORITHMS

Perhaps the most important factor that has allowed Lamb wave techniques to flourish recently is the development of wavelet analysis. Wavelet decomposition is similar to the Fourier decomposition, however instead of just using sines and cosines, complex "mother wavelets" are used to break down the signal [16]. The idea for the wavelet decomposition was first presented by Haar in 1910, however the square wave he used was not very practical for most applications. It was not until 1988 when Daubechies introduced a fractal-like mother wavelet, that the full potential of wavelet analysis for signal decomposition and compression realized. The mother wavelet is essentially used

as an orthogonal basis vector to filter the signal, and is scaled and shifted to approximate the frequency components of the signal. Typically this decomposition is not done continuously since most of the mother wavelets have no closed form solutions. As result a discrete transform on buffered portions of a signal is typically used. This can be performed in commercial software packages such as MATLAB™. Both the present and previous research by the authors used the Morlet wavelet to decompose the signals, since its shape was closest to the driving pulse shape, which makes the processing more accurate and efficient [17]. To analyze the measurements, the Morlet wavelet was scaled between 0 Hz and twice the driving frequency and it was subsequently shifted through the entire time axis. Previously, a simple method was used to distinguish damage using wavelets. Each of these scale bands could be plotted independently to allow observation of the numerical amplitude of signal energy versus time, thus by looking at the central scale band one could filter out all frequencies other than the central driving frequency from the received signals. This provided a clear, filtered view of the transmitted energy from the actuator to the sensors over time, as well as a method of measuring time of flight. The problem with this old method however, was the degree of subjectivity in comparing the levels of energy by eye and distinguishing the true arrival time of the first impinging wavefront. A more thorough method would need to be devised to accurately quantify the damage characteristics present a structure.

In order to accomplish the goals stated above, a new procedure was developed within MATLAB™ to reduce the data resulting from Lamb wave testing. First, a bandpass filter was designed to remove low frequency drift and high frequency electrical noise without affecting signal shape. This custom filter completely removes all frequency components below 1 kHz and above 100 kHz, therefore eliminating signal drift due to air current and higher frequency vibrational and electrical noise. Next, a wavelet decomposition was performed, similar to the one described previously, using Morlet mother wavelet to breakdown signal energy distribution between 7.5-50 kHz. Last, a series of four plots was produced to determine the presence, severity, type and location of the damage. The first plot overlays a cleanly filtered undamaged signal with the signal from the potentially damaged structure. Any deviation from the undamaged signal would indicate that an event has occurred in the structure. The second plot is a comparison of the integrated voltage over time for the undamaged and damaged signals, yielding total received energy to determine the severity of damage. The worse the damage mode, the more energy that would become dispersed and attenuated in the structure, thus yielding a measure of degree of damage. The third plot is of the normalized wavelet energy at driving frequency of 15 kHz to determine time of arrival thus damage location. This was determined to be the most consistent method of measuring time of flight of a Lamb wave, between peaks of highest energy. In order to determine the location of damage accurately, four sets of data would be required—both the transmitted and reflected measurements from either side of the damage, therefore giving an estimate of damage position and geometry. Lastly, the fourth plot shows a comparison of normalized energy received across the entire wavelet spectrum for both the undamaged and damaged signals to determine type of damage. While propagating even through an undamaged structure, a Lamb wave disperses thereby contributing to a small bandwidth of frequencies around the driving frequency. Various types of damage would have different effects on the wavelet spectrum energy, either shifting the central peak, widening the bandwidth or perhaps even causing a secondary peak.

To demonstrate the use of this damage decomposition algorithm, preliminary experimental results using the method described above can be seen in **Figure 7**. These plots were selected from a series of experiments performed using the setup described in the previous sections, which will be further reported upon completion in a future publication. The figures show series of plots that demonstrate the consistency of this setup within undamaged specimens. First, **Figure 7a** demonstrates the repeatability of setting-up and propagating a wave between the same set of actuators and sensors multiple times. Next, **Figure 7b** shows that the signal shape and other parameters remain unchanged when regardless of which side of the damage the signal is sent and received from (while looking only at the transmitted signal). **Figure 7c** exhibits a similar response across several different pairs of equally spaced actuators and sensors on same plate. Lastly, a close response can be seen in **Figure 7d** between pairs of actuators and sensors located on separate undamaged plates. Any deviation is likely due to slight misalignment of the piezoceramic pairs since they are only evident in the signal shape. The next couple figures were included to exemplify the effect of damage on these signals. When a Teflon delamination was present in a specimen, shown in **Figure 7e** the signal was significantly time-lagged, and had a slightly lower energy content. The frequency bandwidth however remained the same. In a specimen with some matrix cracking, shown in **Figure 7f**, a slight time delay was caused, with less energy present after the initial peak, and a small shift to a higher frequency was observed in the bandwidth plot. These are only representative results to demonstrate the effectiveness of this method, however the initial result has been that this overall setup has increased

the signal strength by nearly a factor of four over the previous configurations. Again, with system power increasing with the square of voltage, being able to test at ¼ of the voltage amplitude would decrease the system power requirements by $^1/_{16}$. Work is currently continuing to refine this method using a large set of collected data, however this four-plot method provides a clear path to eventual automation by eliminating human subjectivity from the damage decomposition process and introducing quantifiable figures of merit in its place.

6. FUTURE RECOMMENDATIONS

Lamb wave techniques have good potential for implementation in a SHM system. It can be applied to a structure with conformable piezoelectric devices. The major disadvantage of this method is that it is active; it requires a voltage supply and function generating signal to be supplied. Another difficult requirement is the high data acquisition rate needed to gain useful signal resolution. In order to conserve power and data storage space, the Lamb wave method should most likely be placed into a SHM system in conjunction with another passive detection method, such as a frequency response method. Three to four piezoelectric multi-functioning actuator/sensor patches would be placed in the same vicinity in order to be able to triangulate damage location based upon reciprocal times of flight and reflected waves. Another possible scheme could rely on long strips of piezoelectric material, which would be able to send and receive large uniform Lamb waves, and integrate the received and reflected energy in order to determine the state of the material between them. This paper discusses the optimization of the piezoceramic actuators and sensors for Lamb wave methods, however several other components must be researched further to produce a fully functional SHM system. These components include the batteries, wireless communication and local storage device as well as concepts for robust packaging. Metis Design hopes to address each of these issues over the course of the next few years.

7. CONCLUSIONS

This paper has explored the optimization of actuator and sensor configurations for Lamb wave methods, with applications for damage detection in composite materials. Theoretical calculations were performed to select the appropriate piezoceramic material types and their geometries, as well as for the necessary mechanical and electrical connections. Subsequently, experiments were performed to further verify these calculations, and finalize the configuration for testing. Lastly, a new algorithm was described to decompose and interpret the collected Lamb wave data, and a path towards automated testing was provided. Lamb wave methods have the potential to provide more information than previously tested methods such as frequency response methods since they are more sensitive to the local effects of damage in a structure. The disadvantage of Lamb wave methods is that they require an active driving mechanism to propagate the waves, and the resulting data can be more complicated to interpret than for many other techniques. Overall however, Lamb wave methods have been found to be the most effective for the in-situ determination of the presence, severity and type of damage in composite materials of the methods examined during this research project, and holds the potential to detect the location of damage in a structure. Integrated reliable SHM systems in composite structure will be an important component in future designs of air and spacecraft to increase the feasibility of their missions, and Lamb wave techniques will likely play a role in these systems.

ACKNOWLEDGEMENTS

This research was sponsored by the National Reconnaissance Office, Office of Space Launch, under BAA contract number NRO000-02-C-0625. The work was performed at the Metis Design Corporation in Cambridge, MA, with a subcontract to the Technology Laboratory for Advanced Composites (TELAC) in the Department of Aeronautics and Astronautics at MIT.

REFERENCES

1. Hall S.R. and T.J. Conquest. "The Total Data Integrity Initiative—Structural Health Monitoring, The Next Generation." Proceedings of the USAF ASIP, 1999. 2nd ed.
2. Neumair M. "Requirements on Future Structural Health Monitoring Systems." *Proceedings of the 7th RTO Meetings*, May 1998.
3. Kessler S.S. "Piezoelectric-Based In-Situ Damage Detection of Composite Materials for Structural Health Monitoring Systems." Massachusetts Institute of Technology, Ph.D. thesis, January 2002.
4. Kessler S.S., Spearing S.M., Atalla M.J., Cesnik C.E.S. and C. Soutis. "Damage Detection in Composite Materials using Frequency Response Methods." *Proceedings of the SPIE's 8th International Symposium on Smart Structures and Materials*, 4-8 March 2001, Newport Beach, CA, NDE 4336-01.
5. Kessler S.S., Spearing S.M., Atalla M.J., Cesnik, C.E.S. and C. Soutis. "Structural Health Monitoring in Composite Materials using Frequency Response Methods." Composites Part B, v.33, January 2002, 87-95.
6. Kessler S.S., Spearing, S.M. and C. Soutis. "Damage Detection in Composite Materials using Lamb Wave Methods." *Proceedings of the American Society for Composites*, 9-12 September 2001, Blacksburg, VA.
7. Kessler S.S., Spearing S.M. and C. Soutis. "Optimization of Lamb Wave Methods for Damage Detection in Composite Materials." Proceedings of the 3rd International Workshop on Structural Health Monitoring, 12-14 September 2001, Stanford University.
8. Kessler S.S., Spearing S.M. and C. Soutis. "Structural Health Monitoring in Composite Materials using Lamb Wave Methods." Smart Materials and Structures, v.11, April 2002, 269-278.
9. Kessler S.S., and S.M. Spearing. "Design of a PiezoElectric Based Structural Health Monitoring System for Damage Detection in Composite Materials*." Proceedings of the SPIE's 9th International Symposium on Smart Structures and Materials*, March 2002, San Diego, CA.
10. Kessler S.S., and S.M. Spearing. "In-Situ Sensor-Based Damage Detection of Composite Materials for Structural Health Monitoring Systems." *Proceedings of the AIAA/ASME 43rd Structures, Structural Dynamics and Materials Conference*, April 2002, Denver, CO.
11. Kessler S.S., Spearing S.M., and M.J. Atalla. "In-Situ Damage Detection of Composite Materials using Lamb Wave Methods." Proceedings of the 1st European Workshop on Structural Health Monitoring, July 2002, Paris, France.
12. Lamb H. "On Waves in an Elastic Plate." *Proceedings of the Royal Society of London, Part A: Containing Papers of a Mathematical and Physical Character*, v.93, n.651, 1917, 293-312.
13. Viktorov I.A. *Rayleigh and Lamb Waves, Physical Theor*. Plenum Press, New York, 1967.
14. Nayfeh A.H. *Wave Propagation in Layered Anisotropic Media with Applications to Composites*. v.39, Elsevier, Amsterdam, 1995.
15. Crawley E.F. and J. deLuis. "Use of Piezoelectric Actuators as Elements of Intelligent Structures." *AIAA/ASME 27th Structures, Structural Dynamics and Materials Conference,* San Antonio, Texas , 1986.
16. Strang G. and T. Nguyen *Wavelets and Filter Banks*. Wellesley-Cambridge Press, Wellesley, Ma, 1996.
17. Marantidis C., Van Way C. and J. Kudva. "AE Sensing in an On-Board Smart SHM System for Aircraft." *Proceedings of the SPIE Conference on Smart Structures and Integrated Systems*, v. 2191, 1994, 258-264.

Material	k_P	s_{11}^E	s_{12}^E	σ^P	ε_{33}^P	e_{31}^P
	(-)	(p m^2 / N)	(p m^2 / N)	(-)	(nF/m)	(N / m V)
EBL#23	0.750	15.7	-4.9	0.31	14.7	-29.6
PZT-5K	0.650	16.0	-5.1	0.32	29.6	-29.5
PZT-5M	0.630	15.0	-4.7	0.31	21.5	-26.1
EBL#3	0.640	15.6	-4.6	0.29	18.0	-23.9
PZT-5H	0.635	16.9	-5.1	0.30	17.4	-22.4
PZT-5J	0.630	16.0	-4.7	0.29	14.1	-20.3
PZT-5B	0.640	14.7	-4.3	0.29	12.3	-20.3
EBL#6	0.630	20.3	-6.3	0.31	14.7	-18.6
EBL#25	0.630	22.3	-12.2	0.55	9.6	-17.7
EBL#9	0.600	12.3	-4.4	0.36	8.2	-17.1
PZT-5R	0.630	15.7	-4.0	0.25	10.9	-17.1
EBL#2	0.620	15.1	-4.9	0.33	9.4	-17.0
PZT-5A	0.600	16.1	-5.6	0.35	9.7	-16.8
EBL#1	0.600	10.8	-3.0	0.28	7.4	-16.3
PZT-4	0.580	12.4	-3.9	0.31	7.6	-14.7
EBL#7	0.560	10.8	-3.3	0.31	6.7	-14.3
PZT-7D	0.510	11.8	-3.6	0.31	8.4	-13.7
EBL#4	0.520	10.1	-2.9	0.29	6.8	-13.2
PZT-8	0.520	12.8	-1.2	0.09	6.8	-11.0
EBL#5	0.520	10.6	-3.6	0.33	2.7	-8.5
PZT-7A	0.510	10.6	-3.3	0.31	2.6	-8.2
BT	0.260	7.8	-2.6	0.33	9.1	-8.1

Figure 3: Piezoceramic actuator material figures-of-merit

Material	k_{31}	d_{31}	g_{31}	Y_{11}^D	$\lvert (k_{31})^2/(d_{31}(1-(k_{31})^2)) \rvert$
	(-)	(p m / V)	(mV m / N)	(GPa)	V / (mm με)
PZT-7A	-0.300	-60	-16.2	104	1.65
EBL#5	-0.300	-60	-16	103	1.65
EBL#1	-0.360	-127	-10.7	106	1.17
EBL#7	-0.330	-107	-10.9	104	1.14
EBL#4	-0.310	-95	-10.5	110	1.12
PZT-8	-0.350	-127	-12.2	89	1.10
PZT-4	-0.340	-125	-10.6	91	1.05
EBL#9	-0.340	-135	-10.5	92	0.97
PZT-7D	-0.300	-112	-9.6	94	0.88
PZT-5R	-0.385	-200	-11.5	75	0.87
EBL#2	-0.360	-173	-11.5	76	0.86
PZT-5B	-0.380	-210	-10.1	79	0.80
PZT-5A	-0.343	-177	-11.1	71	0.75
EBL#23	-0.440	-320	-9	79	0.75
PZT-5J	-0.375	-230	-9.8	73	0.71
EBL#3	-0.380	-262	-8.6	75	0.64
PZT-5H	-0.375	-264	-8.9	69	0.62
EBL#6	-0.370	-260	-9.8	57	0.61
PZT-5M	-0.370	-270	-7.6	78	0.59
EBL#25	-0.300	-179	-11	49	0.55
PZT-5K	-0.380	-323	-6.9	73	0.52
PT2/PC6	-0.030	-3	-2.1	135	0.30

Figure 1: Piezoceramic sensor material figures-of-merit

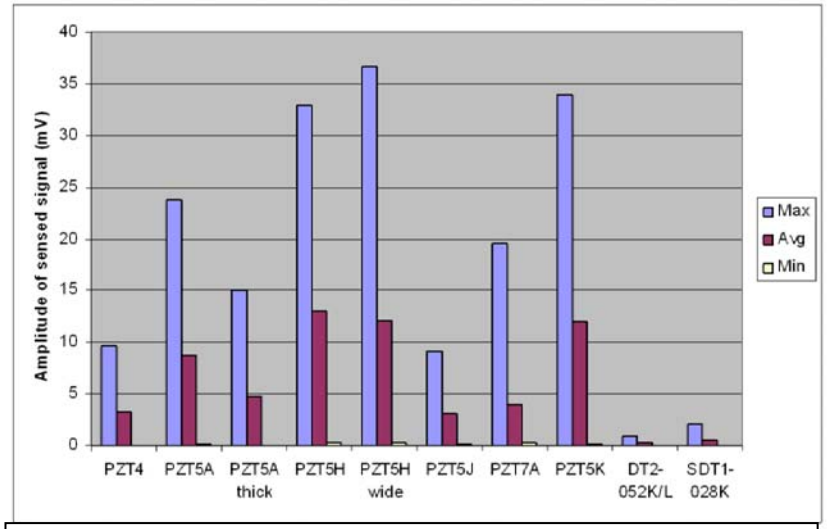

Figure 4: Piezoceramic actuator material test results

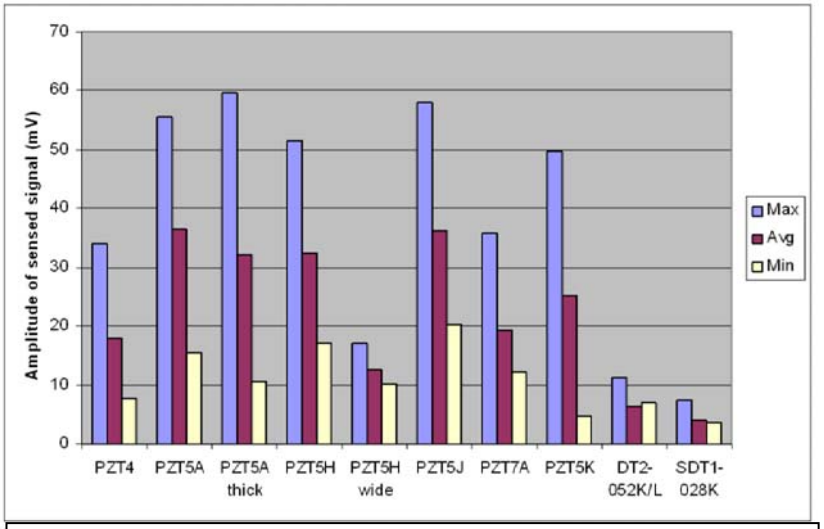

Figure 2: Piezoceramic sensor material test results

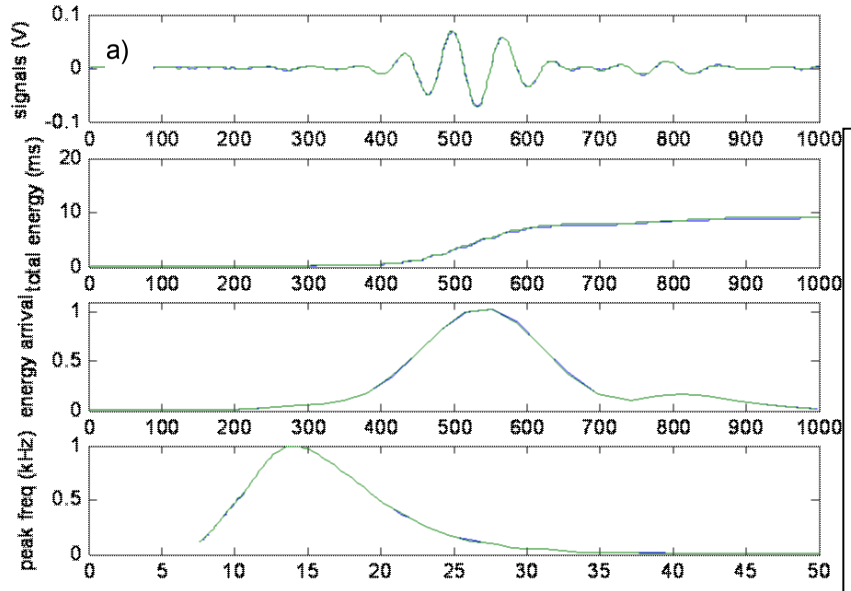

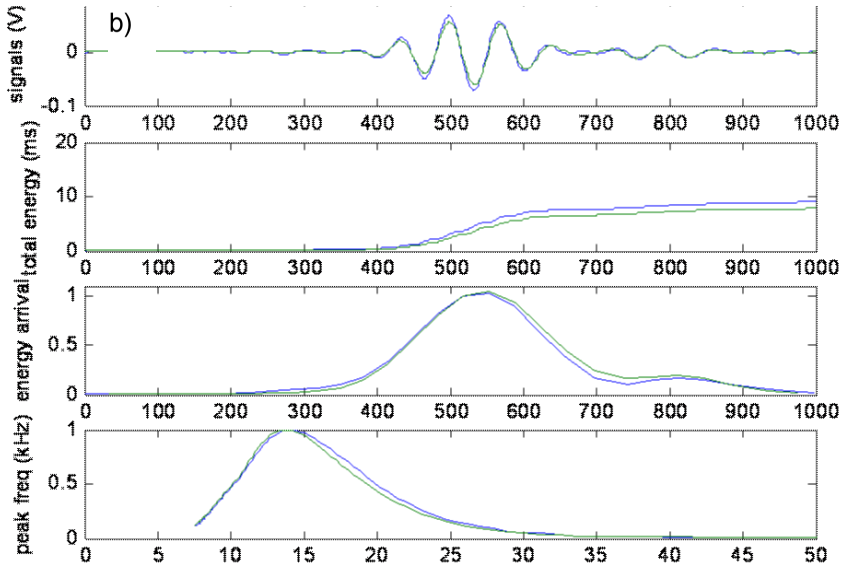

Figure 7: Decomposed signals from undamaged specimens:
a) same sensor se t tested twice; b) sensor set tested forward and reversed

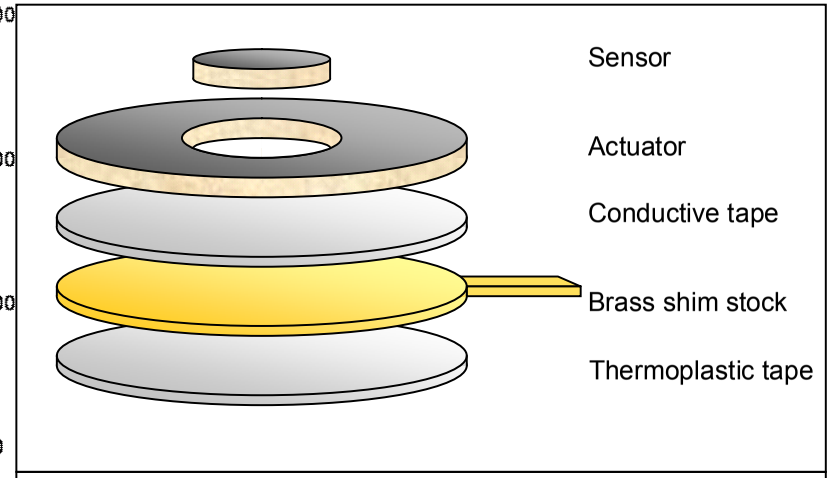

Figure 5: Schematic of complete actuator, sensor, and adhesive assembly

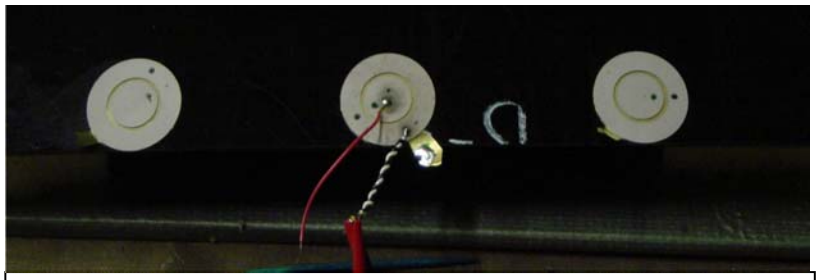

Figure 6: CFRP plate with piezoceramic actuator and sensor assembly

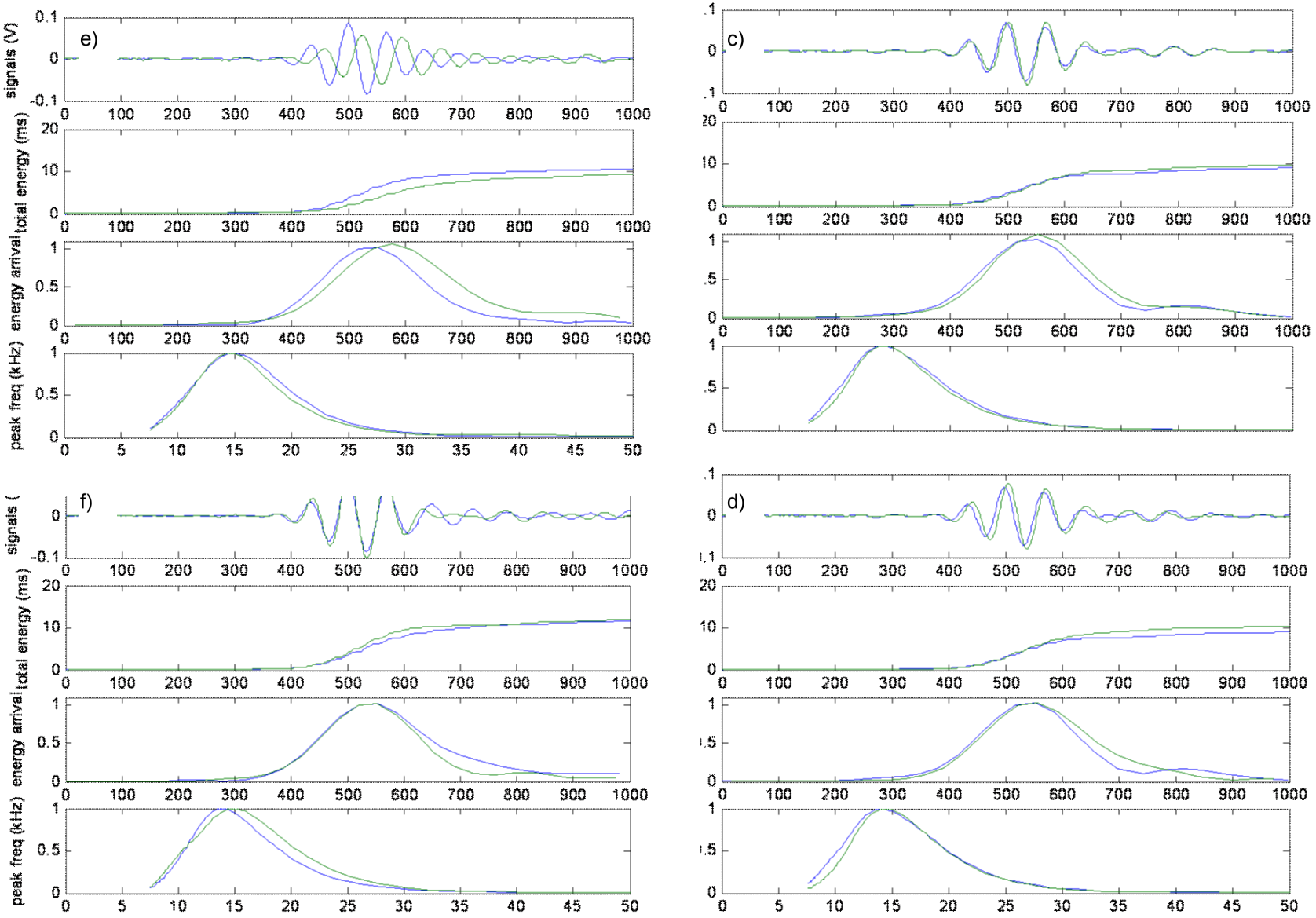

Figure 7 continued: Decomposed signals from damaged undamaged specimens:
c) two sets of sensors on one specimen; d) sensor sets on different specimens; e) delaminated specimen signal; f) microcracked specimen signal